

# Production of $B_s^{(*)}$ Meson induced by the heavy quarks inside the collision hadrons

Jia-Wei Zhang, Xing-Gang Wu,\* Tao Zhong, Yao Yu, Jun Jiang, and Zhen-Yun Fang

*Department of Physics, Chongqing University,  
Chongqing 400044, People's Republic of China*

(Dated: December 7, 2010)

## Abstract

As argued in the literature, the heavy quark components in the collision hadrons may also provide sizable contributions to the hadronic production of the heavy flavored hadrons. Then, different to the fixed-flavor-number scheme (FFNS) as adopted in Ref.[16], we study the hadronic production of  $B_s$  and  $B_s^*$  mesons under the general-mass variable-flavor-number scheme (GM-VFNS) so as to consistently deal with the double counting problem from the two mechanisms, i.e. the extrinsic bottom mechanism via the subprocess  $g + \bar{b} \rightarrow B_s^{(*)} + \bar{s}$  and the gluon-gluon fusion mechanism via the subprocess  $g + g \rightarrow B_s^{(*)} + b + \bar{s}$ . A comparative study of FFN and GM-VFN schemes are presented. At the TEVATRON, the difference between the two schemes is small, however such difference is obvious at the LHC, so the forthcoming experimental data on LHC shall provide a good chance to check which scheme is more appropriate to deal with the  $B_s$  meson production.

**PACS numbers:** 12.38.Bx, 12.39.Jh, 14.40.Ev, 14.40.Nd.

**Keywords:** hadronic production, extrinsic bottom mechanism,  $B_s^{(*)}$  meson, GM-VFN scheme

---

\* wuxg@cqu.edu.cn

## I. INTRODUCTION

The properties of  $B_s$  meson, such as  $B_s - \bar{B}_s$  oscillation, the mass difference  $\Delta m_s$  and the charge-parity violation and etc., have been studied by CDF and D0 collaborations [1–4]. Especially, the CERN LHC, with a high collision energy and a high luminosity, shall provide a good platform for studying the properties of  $B_s$  meson [5, 6]. In the present paper, we shall focus our attention on its hadronic production.

Principally, there are two approaches to deal with the heavy meson hadroproduction. One is the ‘fragmentation approach’, which is usually adaptable to higher transverse momentum region, e.g. Refs.[7–12] showed explicit examples for  $B_c$  hadroproduction and  $B$ -meson hadroproduction respectively. The other one is the so-called ‘complete calculation approach’. Due to the fact that all the phase-space point can be conveniently retained within the ‘complete calculation approach’, while the phase-space of the accompanied particles has been integrated out within the fragmentation approach so as to obtain the fragmentation function. Then the advantage of the complete approach is clear, i.e. it can retain the information of the accompanied quark jets, which sometimes is experimentally useful. Later on, we shall adopt the ‘complete calculation approach’ for our discussions.

In the higher transverse momentum and smaller rapidity regions of a hadronic collider, which mainly corresponding to larger momentum fraction of the constitute quarks, it is found that the heavy quark components in proton or antiproton is always quite small in comparison to that of the light quarks or gluons. So in the literature, one usually does not take heavy quark components’ contributions into consideration in most of the calculations for the heavy quarkonium production. For the purpose, the fixed-flavor-number scheme (FFNS) is usually adopted [13–15]. Within FFNS, the number of the active flavors in the initial hadron is fixed to be  $n_f = 3$ , and then only light quarks/antiquarks and gluon should be considered in the initial state of the hard scattering subprocess. We have studied the hadronic production of the spin-singlet  $B_s$  and the spin-triplet  $B_s^*$  within the ‘complete calculation approach’ by adopting FFNS [16].

However, it has been argued that in certain cases the heavy quark components in the collision hadrons may also provide sizable contributions. For example, it has been shown that the mechanisms involving heavy quarks in the initial state can give sizable contributions to the hadronic production of  $(c\bar{c})$ -quarkonium [17],  $(c\bar{b})$ -quarkonium [18],  $\Xi_{cc}$ -baryons [19, 20],

and etc.. Especially, it is found that in the lower  $p_T$  region, the mechanisms from those heavy quarks in the initial state (hereafter refer to as “heavy quark mechanism”) can even dominant over other mechanisms. The heavy-flavored quarks can be generated in two different ways inside the incident hadrons: firstly, it can be perturbatively generated by gluon splitting, and hence is usually named as ‘extrinsic’ component; and secondly, it can also be generated non-perturbatively and appears at or even below the energy scale of heavy quark threshold that can be named as ‘intrinsic’ one according to Refs.[21, 22]. For the present case of  $B_s^{(*)}$  production, the intrinsic  $b$ -quark component in the hadron is quite small [23], and it shall lead to negligible contribution for the production at both the hadronic colliders TEVATRON and LHC, so we shall not consider it at the present. While, as a comprehensive analysis of the hadronic production of  $B_s^{(*)}$ , it would be interesting to study the extrinsic heavy quarks’ contributions, which might be sizable, and also to make a comparison of the results with those obtained from FFNS.

For such purpose, one has to deal with the production of  $B_s^{(*)}$  through the heavy quark mechanism and the gluon-gluon fusion mechanism simultaneously. This is not an easy task, since we has to solve the double counting problem [24]: i.e. a full QCD evolved heavy quark distribution functions, according to the Altarelli-Parisi equations, includes all the terms proportional to  $\ln\left(\frac{\mu^2}{m_Q^2}\right)$  ( $\mu$  stands for the factorization scale and  $m_Q$  is the heavy quark mass), while some of them also occur in the gluon-gluon fusion mechanism after doing the phase-space integration. We shall adopt the the general-mass variable-flavor-number scheme (GM-VFNS) [25–29] to deal with the double counting problem. It should be noted that our present main purpose is to deal with the double counting problem between the heavy quark mechanism and the gluon-gluon fusion mechanism, and a full NLO calculation of the process is not available at the present due to its complexity, so our present implementation of GM-VFNS is similar to the Aivazis-Collins-Olness-Tung (ACOT) approach [25].

The paper is organized as follows. In Sec.II, we present the calculation technology to estimate the  $B_s^{(*)}$  hadroproduction under the GM-VFNS. In Sec.III, we present our numerical results and a comparison of the hadronic production of  $B_s^{(*)}$  meson from the FFNS and the GM-VFNS shall also be presented. The final section is reserved for a summary.

## II. CALCULATION TECHNOLOGY

According to pQCD factorization theorem, the cross-section for the hadronic production of  $B_s^{(*)}$  under the GM-VFNS can be formulated as

$$\begin{aligned}
d\sigma = & F_{H_1}^g(x_1, \mu) F_{H_2}^g(x_2, \mu) \bigotimes d\hat{\sigma}_{gg \rightarrow B_s^{(*)}}(x_1, x_2, \mu) \\
& + \sum_{i,j=1,2; i \neq j} F_{H_i}^g(x_1, \mu) \left[ F_{H_j}^{\bar{b}}(x_2, \mu) - F_{H_j}^g(x_2, \mu) \bigotimes F_g^{\bar{b}}(x_2, \mu) \right] \bigotimes d\hat{\sigma}_{g\bar{b} \rightarrow B_s^{(*)}}(x_1, x_2, \mu) \\
& + \dots,
\end{aligned} \tag{1}$$

where the ellipsis stands for the terms in higher  $\alpha_s$  order and those terms with smaller contributions, such as the light quark and light anti-quark collision mechanism. The first term in Eq.(1) shows the gluon-gluon fusion mechanism, which is dominant one under the FFNS. The second one represents the extrinsic  $b$ -quark mechanism, in which the subtraction term is introduced to eliminate the double counting problem. The function  $F_H^i(x, \mu)$  (with  $H = H_1$  or  $H_2$  and  $x = x_1$  or  $x_2$ ) stands for the distribution function of parton  $i$  in hadron  $H$ .  $d\sigma$  stands for the hadronic cross-section and  $d\hat{\sigma}$  stands for the corresponding subprocesses. As conventional treatment, we have taken the renormalization scale  $\mu_R$  for the subprocess and the factorization scale  $\mu_F$  for factorizing the PDFs and the hard subprocess to be the same, i.e.  $\mu_R = \mu_F = \mu$ . In the square brackets, the subtraction term for  $F_H^{\bar{b}}(x, \mu)$  is defined as

$$\begin{aligned}
F_H^{\bar{b}}(x, \mu)_{SUB} &= F_H^g(x, \mu) \bigotimes F_g^{\bar{b}}(x, \mu) \\
&= \int_x^1 F_g^{\bar{b}}(\kappa, \mu) F_H^g\left(\frac{x}{\kappa}, \mu\right) \frac{d\kappa}{\kappa},
\end{aligned} \tag{2}$$

where the quark distribution  $F_g^{\bar{b}}(x, \mu)$  up to order  $\alpha_s$  is connected to the familiar  $g \rightarrow b\bar{b}$  splitting function  $P_{g \rightarrow \bar{b}}$ , and its form can be written as

$$F_g^{\bar{b}}(x, \mu) = \frac{\alpha_s(\mu)}{4\pi} (1 - 2x + 2x^2) \ln \frac{\mu^2}{m_b^2}. \tag{3}$$

As for the gluon-gluon fusion mechanism, we need to deal with 36 Feynman diagrams at the leading order ( $\alpha_s^4$ ), which has been dealt with in Ref.[16] by using the improved helicity amplitude approach as described in detail in Ref.[30]. As for the extrinsic  $b$ -quark mechanism for the hadronic  $B_s^{(*)}$  production, we need to consider the production via the subprocess  $g(p_2) + \bar{b}(p_1) \rightarrow B_s^{(*)}(p_3) + \bar{s}(p_4)$ , whose typical Feynman diagrams for the extrinsic  $b$ -quark

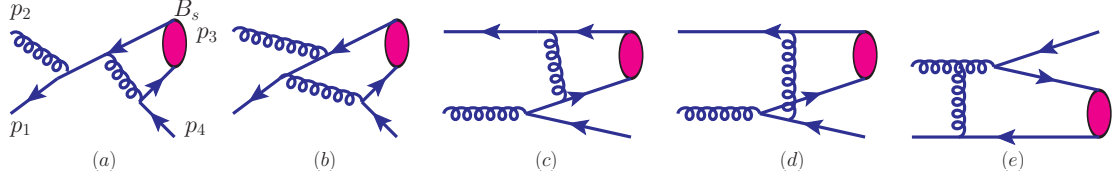


FIG. 1. Typical Feynman diagrams for the heavy quark mechanism, i.e. hadroproduction of  $B_s^{(*)}$  via the subprocesses:  $g(p_2) + \bar{b}(p_1) \rightarrow B_s^{(*)}(p_3) + \bar{s}(p_4)$ .

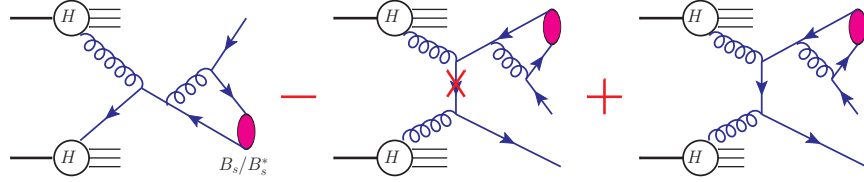


FIG. 2. Graphical representation for the subtraction method within the GM-VFNS [25]. The symbol  $\times$  on the internal quark line in the subtraction term indicates that it is close to the mass-shell and collinear to the gluon and hadron momentum. The combination of the first and the second terms are called as extrinsic mechanism.

mechanism at the leading order (LO) are shown in Fig.(1). In Eq.(1),  $d\hat{\sigma}_{g\bar{b} \rightarrow B_s^{(*)}\bar{s}}(x_1, x_2, \mu) = d\hat{\sigma}_{g\bar{b} \rightarrow B_s^{(*)}\bar{s}}(x_1, x_2, \mu)$  stands for the usual 2-to-2 differential cross section,

$$d\hat{\sigma}_{g\bar{b} \rightarrow B_s^{(*)}\bar{s}}(x_1, x_2, \mu) = \frac{(2\pi)^4 |\overline{M}|^2}{4\sqrt{(p_1 \cdot p_2)^2 - p_1^2 p_2^2}} \prod_{i=3}^4 \frac{d^3 \mathbf{p}_i}{(2\pi)^3 (2E_i)} \delta\left(\sum_{i=3}^4 p_i - p_1 - p_2\right), \quad (4)$$

where the initial-parton spin and color average and the final-state quantum number summation are all attributed to  $|\overline{M}|^2$ .  $|\overline{M}|^2$  can be calculated by using the conventional way, only one needs to keep the heavy quark mass terms according to the GM-VFN scheme. For shortening the text, we do not put  $|\overline{M}|^2$  here, whose explicit form can be found in the APPENDIX of Ref.[18] by simply changing  $m_c$  there to be the present case of  $m_s$ . Next, to accomplish the phase space integration, we adopt two routines RAMBOS [31] and VEGAS [32], which together with some reasonable transformations to make them run more effectively can be found in the generators BCVEGPY [30, 33, 34] and GENXICC [35, 36].

GM-VFNS is considered as the most complete framework for pQCD calculations being applicable in all regions of the phase space of hard processes. In particular, such scheme is by now standard in global analysis of PDFs to extract the most precise sets of partons to

be used for physics predictions at the LHC [37]. According to GM-VFNS, there is double counting of the gluon-gluon fusion mechanism and the extrinsic  $b$ -quark mechanism. For the gluon-gluon fusion mechanism, in some of its Feynman diagrams, when the intermediate heavy quark line that is next to the incident gluon is nearly on shell and is collinear to the incident gluon, then it will result in a factor of order  $\alpha_s$  distribution of a quark in a gluon, like Eq.(3). While such factor has already been included in the heavy quark distribution function, so these Feynman diagrams under such particular condition are double counted and must be subtracted. More explicitly, we draw Fig.(2) as an example to graphically illustrate this point, which is similar to the case of hadronic production of heavy quarks [26]. The symbol ( $\times$ ) on the internal quark line in the subtraction term means that the heavy quark is on mass-shell and moving longitudinally.

It should be noted that our present purpose is to deal with the double counting problem between the heavy quark mechanism and the gluon-gluon fusion mechanism, and a full NLO calculation of the process is not available at the present, so our present implementation of GM-VFNS is similar to the Aivazis-Collins-Olness-Tung (ACOT) approach [25], which sometimes is called as a LO generalized  $\overline{MS}$  calculation [27].

### III. NUMERICAL RESULTS AND DISCUSSIONS

In doing the numerical calculation, we take the decay constant and the radial wave function at the origin to be  $f_{B_s^{(*)}} = 0.209\text{GeV}$  and  $|R(0)|^2 = 0.497\text{GeV}^3$  [38, 39]. The masses of  $b$  and  $s$  quarks are taken as  $m_b = 4.90\text{GeV}$  and  $m_s = 0.50\text{GeV}$ . And to ensure the gauge invariance of the hard scattering amplitude, the mass of the bound state is taken to be the sum of the two constitute quark masses, i.e.  $M_{B_s^{(*)}} = m_b + m_s$ . The scale  $\mu$  is set to be the transverse mass of the bound state, i.e.  $\mu = M_t \equiv \sqrt{M_{B_s^{(*)}}^2 + p_T^2}$ , where  $p_T$  is the transverse momentum of the bound state. Under the GM-VFN scheme, CTEQ6HQ [40] is adopted for PDF, and to be consistent, the NLO  $\alpha_s$  running above  $\Lambda_{QCD}^{(n_f=4)} = 0.326\text{ GeV}$  is adopted, i.e.  $\alpha_s(\mu^2) = \frac{4\pi}{\beta_0 \ln(\mu^2/\Lambda_{QCD}^2)} \left[ 1 - \frac{2\beta_1}{\beta_0^2} \frac{\ln[\ln(\mu^2/\Lambda_{QCD}^2)]}{\ln(\mu^2/\Lambda_{QCD}^2)} \right]$ , where  $\beta_0 = 11 - 2n_f/3$  and  $\beta_1 = 51 - 19n_f/3$ . As a comparison, for the FFN scheme, the LO  $\alpha_s$  running is adopted. It is noted that for GM-VFNS, the value of  $n_f$  changes with the energy scale.

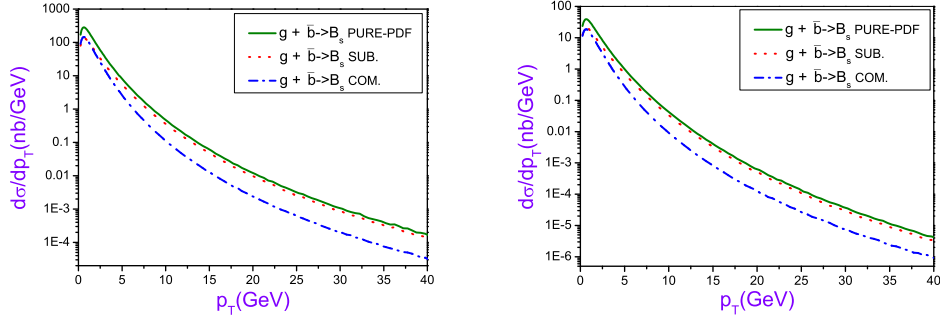


FIG. 3.  $p_T$ -distributions of the extrinsic  $b$ -quark mechanism for the hadronic production of  $B_s$  at LHC (Left) and TEVATRON (Right). The ‘PURE-PDF’ one means the  $b$ -quark PDF is taken to be CTEQ6HQ, ‘SUB.’ one means the  $b$ -quark PDFs is taken to be the subtraction term defined in Eq.(2), ‘COM.’ one stands for the combination of the ‘PURE-PDF’ and ‘SUB.’ components as indicated by Eq.(1).

#### A. Hadroproduction of $B_s^{(*)}$ under the GM-VFNS

Firstly, it would be interesting to show how double counting term is subtracted in GM-VFNS. We present the results of the extrinsic  $b$ -quark mechanism for the hadronic production of  $B_s$  both at LHC and at TEVATRON in Fig.(3). It can be found that there exists a large cancelation between the contributions from the ‘PURE-PDF’ term (with  $b$ -quark PDF taken to be CTEQ6HQ) and the subtraction term (with  $b$ -quark PDF taken to be the subtraction term defined in Eq.(2)), especially, in the large  $p_T$  regions. This shows that to obtain a reliable results under the GM-VFNS, we should take such double counting term into consideration, otherwise, the results maybe largely overestimated.

Secondly, we present the total cross sections for the hadronic production of  $B_s$  and  $B_s^*$  at LHC and TEVATRON, which are shown in Tab.I and Tab.II respectively. Two typical cuts  $p_{Tcut} = 2.5$  GeV and  $p_{Tcut} = 4$  GeV for both LHC and TEVATRON, and  $|y| \leq 1.5$  for LHC,  $|y| \leq 0.6$  for TEVATRON are adopted in the calculation. As a comparison, we also show the results under the FFNS with PDF taken to be CTEQ6L [41] in Tab.I and Tab.II. It should be noted that  $n_f$  should be fixed to be 3 in the FFNS and then to be consistent with the exact FFNS, the PDFs for the initial partons should be taken the one like CTEQ5F3 [42], which is generated by using the evolution kernels with effective flavor

TABLE I. Cross section (in unit  $nb$ ) for the hadronic production of  $B_s$  at LHC ( $\sqrt{s} = 14.0$  TeV) and TEVATRON ( $\sqrt{s} = 1.96$  TeV) under GM-VFNS and FFNS, where the symbol  $g + \bar{b}$  stands for the extrinsic  $b$ -quark mechanism and etc. Two typical  $p_T$  cuts are adopted. As for the rapidity cut, we take  $|y| \leq 1.5$  for LHC and  $|y| \leq 0.6$  for TEVATRON.

-	-	GM-VFN			FFN
	$p_{Tcut}$	$g + \bar{b}$	$g + g$	$total$	$g + g$
LHC	2.5 GeV	14.55	44.43	58.98	83.06
	4.0 GeV	4.41	30.05	34.46	54.39
TEVATRON	2.5 GeV	1.19	3.28	4.48	4.50
	4.0 GeV	0.32	2.05	2.37	2.73

TABLE II. Cross-section (in unit  $nb$ ) for the hadronic production of  $B_s^*$  at LHC ( $\sqrt{s} = 14.0$  TeV) and TEVATRON ( $\sqrt{s} = 1.96$  TeV) under GM-VFNS and FFNS, where the symbol  $g + \bar{b}$  stands for the extrinsic  $b$ -quark mechanism and etc. Two typical  $p_T$  cuts are adopted. As for the rapidity cut, we take  $|y| \leq 1.5$  for LHC and  $|y| \leq 0.6$  for TEVATRON.

-	-	GM-VFN			FFN
	$p_{Tcut}$	$g + \bar{b}$	$g + g$	$total$	$g + g$
LHC	2.5 GeV	32.94	140.0	173.9	265.6
	4.0 GeV	10.45	92.24	102.7	167.9
TEVATRON	2.5 GeV	2.54	10.49	13.03	14.45
	4.0 GeV	0.73	6.33	7.07	8.47

number  $n_{eff} = 3$ . As argued in Refs.[43, 44], the uncertainties from different LO PDFs are small, and our numerically calculation shows that it only gives several percent difference by replacing CTEQ6L to CTEQ5F3 <sup>1</sup>, so as a conventional choice, we also adopt CTEQ6L as the typical PDF for FFNS.

<sup>1</sup> Under FFNS, by varying the flavor number with the energy scale, the value of  $\alpha_s$  shall be decreased, but this is to a large degree compensated by a larger gluon distribution function (i.e. in small  $x$ -region that is dominant for the production,  $F_H^g(\text{CTEQ6L}) > F_H^g(\text{CTEQ5F3})$ ), so as a whole, there is small difference by using CTEQ6L and CTEQ5F3.



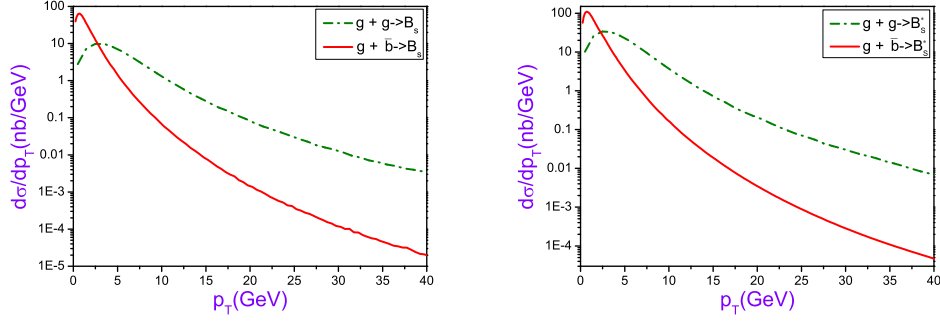


FIG. 4.  $p_T$  distributions for the hadronic production of  $B_s$  (Left) and  $B_s^*$  (Right) at LHC under the GM-VFNS. The dash-dot and the solid lines represent the gluon-gluon fusion mechanism and the extrinsic  $b$ -quark mechanism respectively. All  $p_T$  distributions are drawn under  $|y| < 1.5$  and the PDF is taken as CTEQ6HQ.

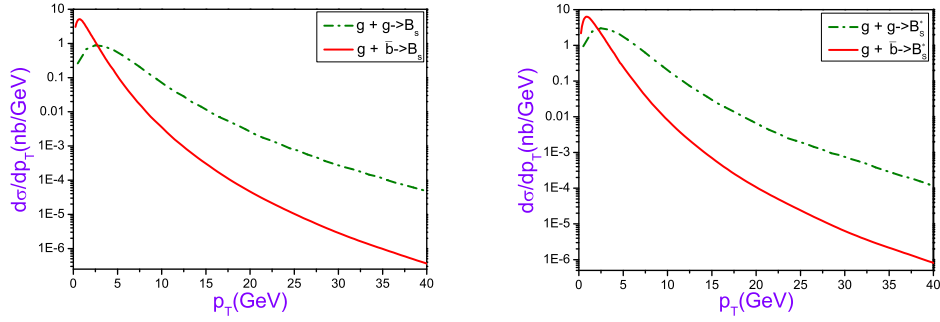


FIG. 5.  $p_T$  distributions for the hadronic production of  $B_s$  (Left) and  $B_s^*$  (Right) at TEVATRON under the GM-VFNS. The dash-dot and the solid lines represent the gluon-gluon fusion mechanism and the extrinsic  $b$ -quark mechanism accordingly. All  $p_T$  distributions are drawn under  $|y| < 0.6$  and the PDF is taken as CTEQ6HQ.

It can be found from Tab.I and Tab.II that the total cross sections of the extrinsic  $b$ -quark mechanism are comparable to those of the gluon-gluon fusion mechanism. The large cross section of the extrinsic  $b$ -quark mechanism mainly comes from the small  $p_T$  region. In order to illustrate this point more clearly, we draw the transverse momentum distributions of  $B_s^{(*)}$  in Figs.(4) and (5), which shows obviously that in a smaller  $p_T$  region, the extrinsic  $b$ -quark mechanism is greater than that of the gluon-gluon fusion mechanism. However it drops down much more quickly with the increment of  $p_T$ , and then in a larger  $p_T$  region,

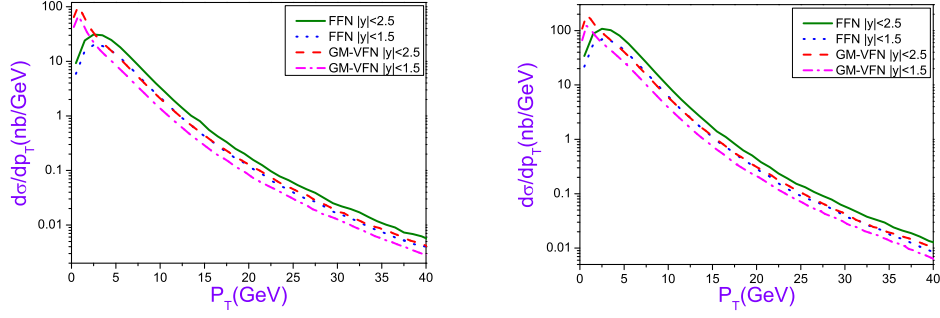


FIG. 6.  $p_T$  distributions for the hadronic production of  $B_s$  (Left) and  $B_s^*$  (Right) at LHC. The dashed and the dash-dotted lines stand for the total (sum of the extrinsic  $b$ -quark mechanism and the gluon-gluon fusion mechanism) results obtained under the GM-VFNS for rapidity cuts  $|y| < 2.5$  and  $|y| < 1.5$  respectively. The solid and the dotted lines are for gluon-gluon fusion results obtained under the FFNS for rapidity cuts  $|y| < 2.5$  and  $|y| < 1.5$  respectively.

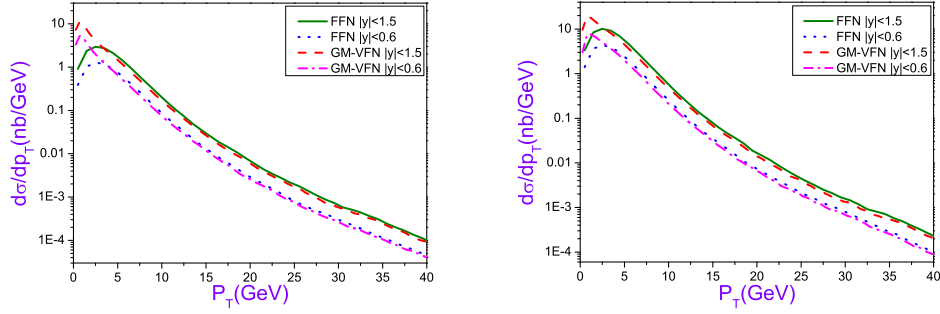


FIG. 7.  $p_T$  distributions for the hadronic production of  $B_s$  (Left) and  $B_s^*$  (Right) at TEVATRON. The dashed and the dash-dotted lines stand for the total (sum of the extrinsic  $b$ -quark mechanism and the gluon-gluon fusion mechanism) results obtained under the GM-VFNS for rapidity cuts  $|y| < 1.5$  and  $|y| < 0.6$  respectively. The solid and the dotted lines are for gluon-gluon fusion results obtained under the FFNS for rapidity cuts  $|y| < 1.5$  and  $|y| < 0.6$  respectively.

the contribution from the extrinsic  $b$ -quark mechanism is lower than that of the gluon-gluon fusion mechanism.

Further more, it can be found that the gluon distribution of CTEQ6HQ is always smaller than that of CTEQ6L, especially in small  $x$  region, so the total cross section for the gluon-

gluon fusion under the GM-VFNS is smaller than that under the FFNS. Since  $x$  may reach to much smaller region at LHC than at TEVATRON, the difference between these two schemes is bigger at LHC than that at TEVATRON. Tab.I and Tab.II show this point clearly. For example for the production of  $B_c$ , when  $p_{Tcut} = 4$  GeV, it can be found that at LHC, the total cross section for the gluon-gluon fusion under the GM-VFNS is only 56% of that of FFNS; while at TEVATRON, such ratio raises up to 75%. This shows that when taking the extrinsic  $b$ -quark mechanism into account for the GM-VFNS, one can shrink the gap between the GM-VFNS and the FFNS results to a certain degree.

It can be found that in the large  $p_T$  region, the extrinsic  $b$ -quark mechanism is greatly suppressed due to the large cancelation from the subtraction term under the GM-VFN scheme, then the contribution from the gluon-gluon fusion mechanism shall be dominant in these higher  $p_T$  regions. In order to see the fact clearly, we present the  $p_T$  distributions predicted by the GM-VFN and FFN schemes for the hadronic production of  $B_s^{(*)}$  at LHC and TEVATRON in Figs.(6) and (7) respectively. Figs.(6) and (7) shows that the main difference between the predictions by the GM-VFNS and the FFNS is only in small  $p_T$  region ( $p_T \lesssim 3.0 \sim 4.0$  GeV). Furthermore, Fig.(7) shows that at TEVATRON, one can hardly distinguish the difference between FFNS and GM-VFNS, since a  $p_{Tcut} \simeq 4\text{GeV}$  is usually adopted at TEVATRON for hadronic productions. This shows that at TEVATRON, FFNS is enough to describe the data. While Fig.(6) shows that at LHC, such difference is amplified, so the forthcoming LHC experiment data may make a judge on whether we need to take the heavy quark component in proton into consideration (and hence the necessity of using GM-VFNS), since more small  $x$  and small  $p_T$  events can be found/measured at LHC.

## B. A simple discussion on the uncertainties from $b$ -quark mass

The uncertainties for the hadronic production of  $B_s$  and  $B_s^*$  include the PDFs, the quark masses, the factorization scale and etc.. We have made a detailed discuss on such uncertainties in Ref.[16] under FFNS, here we shall only concentrate our attention on the  $b$ -quark mass effect on the hadronic production, since the other uncertainties shall give similar behavior under both GM-VFNS and FFNS <sup>2</sup>. For the purpose of discussing the uncertainties

---

<sup>2</sup> We have checked this conclusion numerically, and to short the paper, we do not present extra discussions on other uncertainties.

TABLE III. Cross-section (in unit  $nb$ ) for the hadronic production of  $B_s[1^1S_0]$  at LHC and TEVATRON under GM-VFNS and FFNS with  $m_b$  varying within the region of  $(4.9 \pm 0.1)$  GeV, where the symbol  $g + \bar{b}$  stands for the extrinsic  $b$ -quark mechanism and etc. As for the rapidity cut, we take  $|y| \leq 1.5$  for LHC and  $|y| \leq 0.6$  for TEVATRON. The upper, the center and the lower values are for  $m = 5.0, 4.9$  and  $4.8$  GeV respectively.

-	-	GM-VFN			FFN
-	$p_{Tcut}$	$g + \bar{b}$	$g + g$	$total$	$g + g$
LHC	2.5	$14.55^{+1.30}_{-1.46}$	$44.43^{+2.02}_{-2.15}$	$58.98^{+0.69}_{-0.72}$	$83.06^{+4.51}_{-4.10}$
	4.0	$4.41^{+0.34}_{-0.36}$	$30.05^{+1.02}_{-1.13}$	$34.46^{+0.68}_{-0.77}$	$54.39^{+2.08}_{-2.16}$
Tevatron	2.5	$1.19^{+0.12}_{-0.13}$	$3.28^{+0.18}_{-0.20}$	$4.48^{+0.07}_{-0.07}$	$4.50^{+0.27}_{-0.29}$
	4.0	$0.32^{+0.03}_{-0.03}$	$2.05^{+0.09}_{-0.09}$	$2.37^{+0.06}_{-0.06}$	$2.73^{+0.12}_{-0.13}$

TABLE IV. Cross-section (in unit  $nb$ ) for the hadronic production of  $B_s^*[1^3S_1]$  at LHC and TEVATRON under GM-VFNS and FFNS with  $m_b$  varying within the region of  $(4.9 \pm 0.1)$  GeV, where the symbol  $g + \bar{b}$  stands for the extrinsic  $b$ -quark mechanism and etc. As for the rapidity cut, we take  $|y| \leq 1.5$  for LHC and  $|y| \leq 0.6$  for TEVATRON. The upper, the center and the lower values are for  $m = 5.0, 4.9$  and  $4.8$  GeV respectively.

-	-	GM-VFN			FFN
-	-	$g + \bar{b}$	$g + g$	$total$	$g + g$
LHC	2.5	$32.94^{+2.70}_{-3.04}$	$140.0^{+6.1}_{-6.3}$	$173.9^{+3.3}_{-3.4}$	$265.6^{+12.1}_{-12.8}$
	4.0	$10.45^{+0.76}_{-0.82}$	$92.24^{+2.94}_{-2.96}$	$102.7^{+2.1}_{-2.1}$	$167.9^{+5.3}_{-6.3}$
Tevatron	2.5	$2.54^{+0.23}_{-0.27}$	$10.49^{+0.56}_{-0.60}$	$13.03^{+0.33}_{-0.33}$	$14.45^{+0.89}_{-0.83}$
	4.0	$0.73^{+0.06}_{-0.07}$	$6.33^{+0.25}_{-0.26}$	$7.07^{+0.19}_{-0.20}$	$8.47^{+0.35}_{-0.40}$

caused by  $m_b$ , we vary  $m_b$  within the region of  $(4.9 \pm 0.1)$  GeV. The total cross section for the hadronic production of the scalar  $B_s[1^1S_0]$  and the vector  $B_s^*[1^3S_1]$  at LHC and TEVATRON under GM-VFNS and FFNS are presented in TAB.III and TAB.IV. For definiteness and focussing the uncertainties from the  $b$ -quark mass alone, and we fix  $m_s = 0.5$  GeV,

$m_{B_s} = m_s + m_b$ ,  $\mu_F^2 = p_{T_{B_s}}^2 + m_{B_s}^2$  and the PDF is taken from CTEQ6HQ and CTEQ6L for GM-VFNS and FFNS respectively.

From TAB.III and TAB.IV, it is found that the total cross section for the extrinsic mechanism *increases* with the increment of  $m_b$ . For clarity, in the following, we shall take the case of  $B_s$  as an explicit examples to explain this point, and the case of  $B_s^*$  is similar. When setting  $p_{T_{cut}} = 2.5$  GeV, the total cross section for  $B_s$  shall be *increased* by 10% when  $m_b$  increased by 0.1 GeV at both LHC and TEVATRON, which reduces to be 8% at LHC and 9% at TEVATRON for  $p_{T_{cut}} = 4.0$  GeV. Inversely, since the allowed phase space becomes narrower with the increment of  $m_b$ , it is found that the total cross section for the gluon-gluon fusion mechanism *decreases* with the increment of  $m_b$ . The total cross section of  $B_s$  for the gluon-gluon fusion mechanism shall be *decreased* by 5% (6%) when  $m_b$  increased by 0.1 GeV for  $p_{T_{cut}} \geq 2.5$  GeV at LHC ( at TEVATRON). As a combination, due to the different behavior of the extrinsic mechanism and the gluon-gluon fusion mechanism, the total cross sections under GM-VFNS possess smaller uncertainties in comparison to that of FFNS, which are 1.2% and  $\sim 1.5\%$  at  $p_{T_{cut}} = 2.5$  GeV when  $m_b$  increased by 0.1 GeV at LHC and TEVATRON respectively.

#### IV. SUMMARY

As a compensation of our previous work [16] on the hadronic production of  $B_s^{(*)}$  meson, we have reanalyzed the production under the GM-VFNS, and a comparison with the estimations of FFNS and GM-VFNS is also presented. Under the FFNS, we only need to deal with the dominant gluon-gluon fusion mechanism as done in Ref.[16]. While under the GM-VFNS, in addition to the gluon-gluon fusion mechanism, one also needs to consider the extrinsic heavy quark mechanism so as to make a more sound estimation. For the present case, it is found that the extrinsic  $b$ -quark mechanism can be as important as the gluon-gluon fusion mechanism, especially in small  $p_T$  region. This shows that if the hadronic experiments such as those at LHC and at TEVATRON can accumulate enough data and measure very low  $p_T$  events then they can provide a good platform to check which scheme is more appropriate.

**Acknowledgments:** This work was supported in part by Natural Science Foundation Project of CQ CSTC under Grant No.2008BB0298, by Natural Science Foundation of China

under Grant No.10805082 and No.11075225, and by the Fundamental Research Funds for the Central Universities under Grant No.CDJZR101000616 and No.CDJXS11102209.

- 
- [1] D. Acosta *et al.*, (CDF Collaboration), Phys.Rev. D**71**, 032001 (2005); Phys.Rev. Lett.**94**, 101803 (2005); T. Aaltonen, *et al.*, (CDF Collaboration), Phys.Rev. Lett.**100**, 082001(2008).
  - [2] A. Abulencia*et al.*, (CDF Collaboration), Phys.Rev. Lett.**97**, 062003 (2006); Phys.Rev. Lett. **97**, 242003(2006).
  - [3] V.M. Abazov *et al.*, (D0 Collaboration), Phys.Rev. Lett.**94**, (2005) 042001; Phys.Rev. Lett.**98**, (2007)121801.
  - [4] H.G. Evans, Frascati Phys. Ser.**44**, 421(2007); S. Burdin, arXiv:0707.1509[hep-ph].
  - [5] N. Brambilla *et al.*, Quarkonium Working Group, Published as CERN Yellow Report, CERN-2005-005, arXiv: 0412158[hep-ph].
  - [6] N. Brambilla, *et al.*, Quarkonium Working Group, arXiv:1010.5827.
  - [7] E.Braaten, K. Cheung and T.C. Yuan, Phys.Rev. D **48**, 4230(1993); E. Braaten, K. Cheung and T.C. Yuan, Phys.Rev. D **48**, R5049 (1993);
  - [8] E. Braaten, K. Cheung, S. Fleming and T.C. Yuan, Phys.Rev. D**51**, 4819(1995).
  - [9] J. Binnewies, B.A. Kniehl and G. Kramer, Phys.Rev. D**58**, 034016(1998).
  - [10] M. Cacciari and M. Greco, Nucl.Phys. B**421**, 530(1994).
  - [11] M. Cacciari, S. Frixione, M.L. Mangano, P. Nason and G. Ridolfi, JHEP **0407**, 033(2004).
  - [12] M. Cacciari, M. Greco and P. Nason, JHEP **9805**, 007(1998); M. Cacciari and P. Nason, Phys.Rev. Lett. **89**, 122003(2002).
  - [13] P. Nason, S. Dawson and R.K. Ellis, Nucl.Phys. B**327**, 49(1989).
  - [14] W. Beenakker, H. Kuijf, W.L. Van Neerven and J. Smith, Phys.Rev. D**40**, 54(1989).
  - [15] S. Frixione, M.L. Mangano, P. Nason and G. ridolfi, Adv.Ser.Dir. High Energy Phys. **15**, 609(1998).
  - [16] Jia-Wei Zhang, Zhen-Yun Fang, Chao-Hsi Chang, Xing-Gang Wu, Tao Zhong and Yao Yu, Phys.Rev. D**79**, 114012(2009).

- [17] Cong-Feng Qiao, J. Phys. G**29**, 1075(2003).
- [18] Chao-Hsi Chang, Cong-Feng Qiao, Jian-Xiong Wang and Xing-Gang Wu, Phys.Rev. D**72**, 114009(2005).
- [19] Chao-Hsi Chang, Cong-Feng Qiao, Jian-Xiong Wang and Xing-Gang Wu, Phys.Rev. D**73**, 094022(2006).
- [20] Chao-Hsi Chang, Jian-Ping Ma, Cong-Feng Qiao, Xing-Gang Wu, J.Phys. G**34**, 845(2007).
- [21] S.J. Brodsky, C. Peterson and N. Sakai, Phys. Rev. D**23**, 2745 (1981).
- [22] S.J. Brodsky, P. Hoyer, C. Peterson and N. Sakai, Phys.Lett. B**93**, 451(1980).
- [23] J. Pumplin, Phys.Rev. D**73**, 1140015(2006).
- [24] J. Collins, F. Wilczek and A. Zee, Phys. Rev. D**18**, 242(1978).
- [25] F.I. Olness, R.J. Scalise and W.K. Tung, Phy. Rev. D**59**, 014506(1998).
- [26] M.A.G. Aivazis, J.C. Collins, F.I. Olness and W.K. Tung, Phys. Rev. D**50**, 3102(1994); M.A.G. Aivazis, F.I. Olness and W.K. Tung, Phys. Rev. D**50**, 3085(1994).
- [27] J. Amundson, C. Schmidt, W.K. Tung and X.N. Wang, JHEP**10**, 031(2000).
- [28] B.A. Kniehl, G. Kramer, I. Schienbein and H. Spiesberger, Phys.Rev. D**71**, 014018(2005); Eur.Phys.J. C**41**, 199(2005); Phys.Rev. Lett.**96**, 012001(2006).
- [29] B.A. Kniehl, G. Kramer, I. Schienbein and H. Spiesberger, Phys.Rev. D**77**, 014011(2008).
- [30] Chao-Hsi Chang, Chafik Driouich, Paula Eerola and Xing-Gang Wu, Comput. Phys. Commun. **159**, 192 (2004).
- [31] R. Kleiss and W.J. Stirling, Comput. Phys. Commun, **40** (1986) 359.
- [32] G.P. Lepage, J. Comp. Phys **27**, 192(1978).
- [33] Chao-Hsi Chang, Jian-Xiong Wang and Xing-Gang Wu, Comput.Phys.Commun.**174**, 241(2006).
- [34] Chao-Hsi Chang, Jian-Xiong Wang and Xing-Gang Wu, Comput.Phys.Commun.**175**, 624(2006).
- [35] Chao-Hsi Chang, Jian-Xiong Wang and Xing-Gang Wu, Comput.Phys.Commun.**177**, 467(2007).
- [36] Chao-Hsi Chang, Jian-Xiong Wang and Xing-Gang Wu, Comput.Phys.Commun.**181**, 1144(2010).
- [37] P.M. Nadolsky, *et al.*, Phys.Rev. D**78**, 013004(2008). And references therein.

- [38] Chao-Hsi Chang, Yu-Qi Chen, Phys. Rev. D **49**, 3399(1994); Chao-Hsi Chang and Yu-Qi Chen, Commun. Theor. Phys. **23**, 451(1995).
- [39] E.J. Eichten and C. Quigg, Phys. Rev. D**49**, 5845 (1994); Y.Q. Chen and Y.P. Kuang, Phys. Rev. D**46**, 1165(1992).
- [40] S. Kretzer, H.L. Lai, F.I. Olness and W.K. Tung, Phys. Rev. D**69**, 114005(2004).
- [41] J. Pumplin, D.R. Stump, J. Huston, H.L. Lai, P. Nadolsky and W.K. Tung, JHEP **0207**, 012(2002).
- [42] H. L. Lai, *etal.*, Eur. Phys. J. C**12**,375(2000).
- [43] Chao-Hsi Chang and Xing-Gang Wu, Eur. Phys. J. C**38**, 267(2004).
- [44] Chao-Hsi Chang, Cong-Feng Qiao, Jian-Xong Wang and Xing-Gang Wu, Phys. Rev.D**72**, 114009(2005).